

# In search of the elusive amalgam $\text{SrHg}_8$ : a mercury-rich intermetallic compound with augmented pentagonal prisms†

Andriy V. Tkachuk and Arthur Mar\*

Received 13th April 2010, Accepted 20th May 2010

First published as an Advance Article on the web 14th June 2010

DOI: 10.1039/c0dt00304b

In confirmation of its predicted existence in the Sr–Hg phase diagram, the mercury-rich intermetallic compound  $\text{SrHg}_8$  has been prepared by reaction of the elements at 200 °C. Single-crystal X-ray diffraction analysis revealed that it adopts a new structure type (Pearson symbol  $oP72$ , space group  $Pnma$ ,  $a = 13.328(1)$  Å,  $b = 4.9128(5)$  Å,  $c = 26.446(3)$  Å). The Sr atoms are centred within two types of 18-vertex Hg polyhedra formed by augmenting pentagonal prisms with octagonal waists. The condensation of these  $\text{Sr@Hg}_{18}$  clusters is associated with the formation of a complex anionic Hg–Hg bonding network, as supported by electronic structure calculations which reveal strong mixing of Hg 6s and 6p states in highly delocalized bands superimposed with a narrower 5d band below the Fermi level.

## Introduction

The alloys of mercury, or amalgams, were one of the earliest chemical substances studied by alchemists in their quest for the transmutation to gold. To this day, the existence and structures of many amalgam phases remain undetermined.<sup>1–3</sup> The most systematically investigated amalgams are those of the alkali metals, relatively less is known about the alkaline-earth-metal amalgams, and ternary Li–(Ca, Sr)–Hg phases were only discovered last year.<sup>4</sup>

Over a century ago, the first experiments to elucidate the Sr–Hg phase diagram were carried out, followed by other sporadic attempts.<sup>5–8</sup> The most comprehensive modern re-evaluation of this diagram indicated the existence of several Hg-rich phases, some of whose formulas and structures are still ambiguous, partly because of their extreme air sensitivity and because of difficulties in performing X-ray diffraction analyses.<sup>9</sup> For example, we have recently reformulated the phase “ $\text{Sr}_{14}\text{Hg}_{51}$ ” more properly as  $\text{Sr}_{11-x}\text{Hg}_{54+x}$ , which adopts a crystal structure showing differences from the assumed  $\text{Gd}_{14}\text{Ag}_{51}$ -type.<sup>10</sup> An assessment of the Sr–Hg phase diagram suggested that “ $\text{SrHg}_{13}$ ” should be deleted and that a phase with approximate composition “ $\text{SrHg}_{5-8}$ ” may instead be present.<sup>11</sup>

We report here the discovery of this heretofore missing phase, which is defined by the precise composition  $\text{SrHg}_8$ , and the determination of its crystal structure. The electronic structure was also examined through band structure calculations.

## Results and discussion

$\text{SrHg}_8$  was obtained in the form of air-sensitive silver crystals by reaction of the elements in a Nb tube. Its formation supports the modification, proposed by Gumiński,<sup>11</sup> of the Sr–Hg phase

diagram constructed by Bruzzone and Merlo.<sup>9</sup> In earlier studies,<sup>6–8</sup> this elusive phase was estimated to have a composition of  $\text{SrHg}_{5-8}$ . The conditions of the synthesis performed here (10 at.% Sr, 200 °C) correspond to a two-phase region bounded by a Hg-rich liquid and solid  $\text{SrHg}_8$ , below a peritectic temperature variously reported to be between 262 and 289 °C.<sup>11</sup>

The structure of  $\text{SrHg}_8$  was determined from single-crystal X-ray diffraction (space group  $Pnma$ ,  $Z = 8$ ). The simple formula belies a rather complicated structure (Fig. 1) derived from two Sr and sixteen Hg sites, which are centred within polyhedra

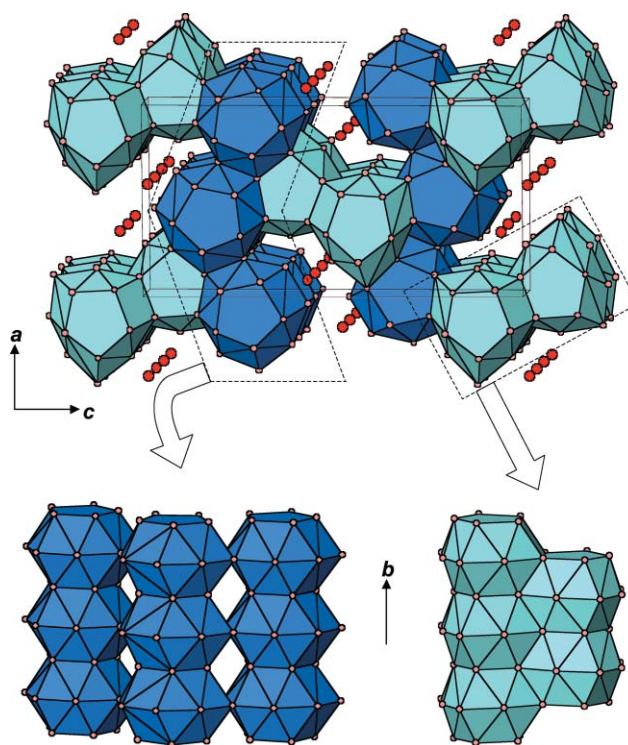


**Fig. 1** Structure of  $\text{SrHg}_8$  in terms of CN18 polyhedra centred by  $\text{Sr}_1$  (dark blue) and  $\text{Sr}_2$  atoms (light blue), with Hg atoms (pink) at the vertices. The voids contain isolated  $\text{Hg}_5$  atoms (red).

Department of Chemistry, University of Alberta, Edmonton, Alberta, Canada T6G 2G2. E-mail: arthur.mar@ualberta.ca; Fax: +1 780 492 8231; Tel: +1 780 492 5592

† Electronic supplementary information (ESI) available: Table of interatomic distances, figure showing additional coordination polyhedra. For ESI and crystallographic data in CIF or other electronic format see DOI: 10.1039/c0dt00304b

with very high coordination numbers (CN). The Sr atoms are surrounded by Hg atoms in two types of 18-vertex polyhedra, described as pentagonal prisms encircled by octagonal waists. These augmented pentagonal prisms are arranged in infinite columns aligned along the *b* direction by sharing the pentagonal faces. The columns of Sr1-centred polyhedra are then condensed together to form slabs lying parallel to the *ab* plane; these slabs are separated by columns of Sr2-centred polyhedra paired together in a staggered fashion. The remaining voids generated by the condensation of these polyhedra are occupied by isolated Hg5 atoms. The Hg atoms are centred within coordination polyhedra of their own, classified as either augmented tetragonal or augmented trigonal prisms (Fig. S1 in the ESI†). These polyhedra, of course, are highly distorted; the descriptions are only meant to be general and the distance cutoffs used (~4.0 Å) may not imply bonding interactions. However, the Hg-centred polyhedra tend to have much lower CN (9–13) than do the Sr-centred ones (18). The Hg–Hg distances (mostly 2.8–3.4 Å, with some longer ones up to 3.8 Å) also tend to be shorter than the Sr–Hg distances (mostly 3.4–3.8 Å, with some longer ones exceeding 4.0 Å). The lower limits of these distances agree well with the sum of the metallic radii (Sr, 1.91 Å; Hg, 1.39 Å).<sup>12</sup> The clear partitioning of the distances is consistent with the absence of disorder between Sr and Hg atoms.

An alternative way to view the structure is in terms of two-dimensional Hg nets stacked along the direction of the short *b* axis (Fig. 2). Adjacent nets (at *y* = 1/4 and *y* = 3/4) are related by a twofold screw axis operation. The nets are made up of triangles, quadrilaterals, pentagons, and octagons. From this perspective, it is easy to see how the two types of Sr coordination polyhedra are formed when a Sr atom is centred on the same plane of an octagon and is sandwiched by pentagons above and below.

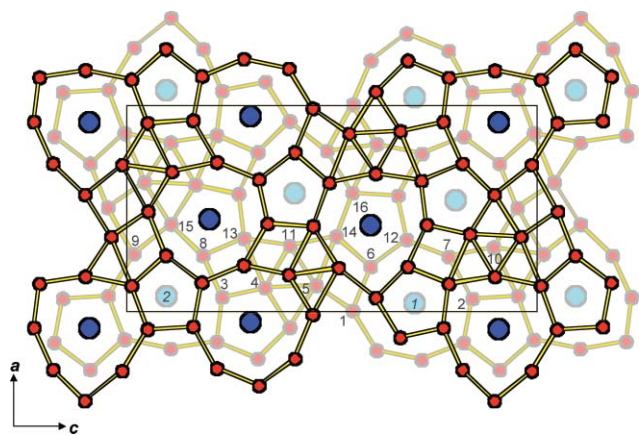


**Fig. 2** Stacking of two-dimensional nets at *y* = 1/4 (lightly shaded) and *y* = 3/4 (heavily shaded). Large blue circles are Sr atoms and small red circles are Hg atoms. Crystallographically unique atoms are labelled.

A search of the literature suggests that SrHg<sub>8</sub> might be related to the recently reported ternary intermetallic compound SrAu<sub>4</sub>In<sub>4</sub>.<sup>13</sup> These compounds are formally isoelectronic and both crystallize in space group *Pnma*, with a doubled *c* parameter in SrHg<sub>8</sub>. However, there is no simple structural relationship between them because the coordination polyhedra surrounding the Sr atoms differ markedly (Fig. 3). In SrHg<sub>8</sub>, the Sr atoms are centred in augmented pentagonal prisms (CN18, with a 5–8–5 arrangement

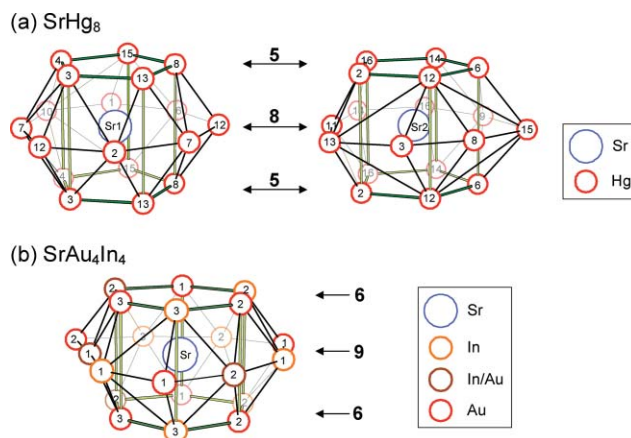


**Fig. 3** Comparison of Sr-centred polyhedra in (a) SrHg<sub>8</sub> and (b) SrAu<sub>4</sub>In<sub>4</sub>.

of parallel planar rings), whereas in SrAu<sub>4</sub>In<sub>4</sub>, they are centred in augmented hexagonal prisms (CN21, with a 6–9–6 arrangement of parallel planar rings) with the vertices made up of Au, In, or mixed Au/In sites. Interestingly, if very long distances (>4.5 Å) are excluded, the effective coordination environment around the Sr atoms in SrAu<sub>4</sub>In<sub>4</sub> is reduced to CN18.<sup>13</sup> Although these polyhedra also condense to form columns along the *b* direction in SrAu<sub>4</sub>In<sub>4</sub>, their connectivity along the other two directions differs substantially from that in SrHg<sub>8</sub>. Presumably, size effects associated with the presence of two electronegative elements (Au, 1.34 Å; In 1.42 Å)<sup>12</sup> are primarily responsible for the more irregular coordination environments and thereby different packing requirements in SrAu<sub>4</sub>In<sub>4</sub> than in SrHg<sub>8</sub>.

Attempting to apply the Zintl concept to mercury intermetallics goes well beyond its traditional limits of validity.<sup>2</sup> Nevertheless, it is sensible to expect that an electropositive alkaline-earth metal in combination with a highly electronegative d-block element (Pauling electronegativities: Sr, 1.0; Hg, 1.9)<sup>12</sup> will lead to partial electron transfer to form a “mercuride”. In a highly Hg-rich compound like SrHg<sub>8</sub>, whatever electron density that is transferred by the Sr atoms will be distributed over a large number of Hg atoms. The calculated density of states curve reveals that the Sr 5s states are mostly unoccupied, lying above the Fermi level (Fig. 4). The filled levels consist mostly of a prominent Hg 5d band that is only slightly broadened (from –9 to –6 eV), superimposed on a very disperse band (from –9 eV upwards) derived from Hg 6s–6p hybridized states. Characteristic of Hg-rich amalgams, this disperse Hg 6s–6p band is associated with Hg–Hg bonding interactions, as reflected in the many distances (as short as 2.8 Å) found in the crystal structure that are comparable to those in elemental Hg (3.00 Å).<sup>14</sup>

## Experimental

### Synthesis

All reagents and products were handled within an Ar-filled glovebox. A 0.25 g mixture of Sr (dendritic pieces, 99.99%, Aldrich) and Hg (99.9999%, Aldrich) in the stoichiometry “Sr<sub>0.10</sub>Hg<sub>0.90</sub>” was placed in a Nb container, which was arc-welded under argon and then sealed within a fused-silica tube under vacuum. Annealing

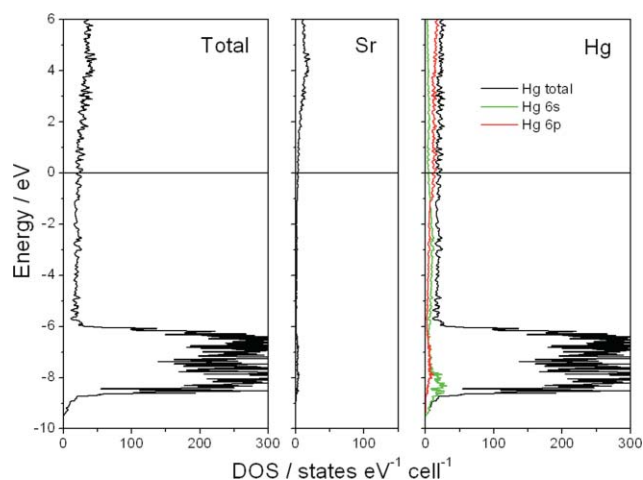


**Fig. 4** Density of states (DOS) for  $\text{SrHg}_8$ , and its Sr and Hg projections. The Fermi level is marked by the horizontal line at 0 eV. In the right panel, the Hg 6s (green) and 6p (red) orbital contributions are plotted.

at 200 °C for 1 month, followed by quenching in cold water, led to the formation of small silver needle-shaped crystals. Elemental compositions could not be determined by usual methods (e.g., EDX analysis) because these crystals are highly air-sensitive.

### Structure determination

A single crystal was selected from the products and mounted on a glass fibre under Paratone-N oil. Single-crystal X-ray diffraction data were collected on a Bruker Platform/SMART 1000 CCD diffractometer at –80 °C using  $\omega$  scans. Structure solution and refinement were carried out with use of the SHELXTL (version 6.12) program package.<sup>15</sup> Face-indexed numerical absorption corrections were essential, given that the absorption coefficient is extremely large ( $\mu(\text{MoK}\alpha) = 141.20 \text{ mm}^{-1}$ ), resulting in very low transmission factors (0.00–0.03). Notwithstanding these difficulties, the identification of the space group ( $Pnma$ ) and the location of the atoms, found by direct methods, were straightforward. Least-squares refinements indicated that the atomic sites are fully occupied by Sr and Hg atoms in an ordered fashion, with reasonable displacement parameters. Atomic positions were standardized with the program STRUCTURE TIDY.<sup>16</sup> Crystal data and further details of the data collections are given in Table 1. Final values of the positional and displacement parameters are given in Table 2. Interatomic distances less than  $\sim 4.0 \text{ \AA}$  are listed fully in Table S1 (ESI†) and in condensed form in Table 3. Further data, in the form of a Crystallographic Information File (CIF), may be obtained from Fachinformationszentrum Karlsruhe, Abt. PROKA, 76344 Eggenstein-Leopoldshafen, Germany (No. CSD-421827).

### Band structure

A tight-binding linear muffin tin orbital (TB-LMTO) band structure calculation was performed on  $\text{SrHg}_8$  within the local density and atomic spheres approximations using the Stuttgart TB-LMTO program.<sup>17</sup> The basis sets consisted of Sr 5s/5p/4d/4f and Hg 6s/6p/5d/5f orbitals, with the Sr 5p/4f and Hg 5f orbitals being downfolded. Integrations in reciprocal space were carried

**Table 1** Crystallographic data for  $\text{SrHg}_8$

Formula	$\text{SrHg}_8$
Formula mass/amu	1692.34
Space group	$Pnma$ (no. 62)
$T/\text{°C}$	–80
$a/\text{\AA}$	13.328(1)
$b/\text{\AA}$	4.9128(5)
$c/\text{\AA}$	26.446(3)
$V/\text{\AA}^3$	1731.6(3)
$Z$	8
$\rho_{\text{calcd}}/\text{g cm}^{-3}$	12.983
Radiation	$\text{Mo K}\alpha$ , $\lambda = 0.71073 \text{ \AA}$
$\mu/\text{mm}^{-1}$	147.28
Transmission factors	0.000–0.030
$2\theta$ range/ $^\circ$	4.34–66.28
No. of data collected	23 190 ( $R_{\text{int}} = 0.174$ )
No. of unique data	3599 (2435 with $F^2 > 2\sigma(F^2)$ )
No. of variables	110
$R(F)$ ( $F^2 > 2\sigma(F^2)$ ) <sup>a</sup>	0.062
$R_w(F^2)$ <sup>b</sup>	0.159
Goodness of fit	1.007
$(\Delta\rho)_{\text{max}}, (\Delta\rho)_{\text{min}}/\text{e \AA}^{-3}$	6.48, –5.38

<sup>a</sup>  $R(F) = \sum \|F_o| - |F_c\| / \sum |F_o|$ ; <sup>b</sup>  $R_w(F^2) = [\sum [w(F_o^2 - F_c^2)^2] / \sum wF_o^4]^{1/2}$ ,  $w^{-1} = [\sigma^2(F_o^2) + (AP)^2 + Bp]$  where  $p = [\max(F_o^2, 0) + 2F_c^2]/3$ .

**Table 2** Positional and equivalent isotropic displacement parameters for  $\text{SrHg}_8$ <sup>a</sup>

Atom	$x$	$z$	$U_{\text{eq}}^b/\text{\AA}^2$
Sr1	0.04625(17)	0.70039(10)	0.0141(5)
Sr2	0.07863(16)	0.09388(9)	0.0120(5)
Hg1	0.00976(10)	0.54912(6)	0.0344(4)
Hg2	0.06793(8)	0.84075(5)	0.0217(3)
Hg3	0.07457(8)	0.22971(5)	0.0230(3)
Hg4	0.12026(8)	0.33523(5)	0.0233(3)
Hg5	0.13229(6)	0.45946(5)	0.0262(3)
Hg6	0.22297(9)	0.59239(6)	0.0277(3)
Hg7	0.27078(8)	0.78285(4)	0.0197(2)
Hg8	0.27714(7)	0.18311(5)	0.0217(3)
Hg9	0.28370(8)	0.01419(4)	0.0215(3)
Hg10	0.31653(9)	0.89290(5)	0.0230(3)
Hg11	0.32499(7)	0.39571(4)	0.0165(2)
Hg12	0.35401(10)	0.68018(5)	0.0260(3)
Hg13	0.35978(9)	0.28367(5)	0.0234(3)
Hg14	0.36980(9)	0.50857(4)	0.0216(3)
Hg15	0.42829(11)	0.10521(5)	0.0316(3)
Hg16	0.58149(8)	0.54791(5)	0.0205(3)

<sup>a</sup> All atoms are in Wyckoff position 4c ( $x, 1/4, z$ ). <sup>b</sup>  $U_{\text{eq}}$  is defined as one-third of the trace of the orthogonalized  $U_{ij}$  tensor.

**Table 3** Ranges of interatomic distances ( $\text{\AA}$ ) in  $\text{SrHg}_8$ <sup>a</sup>

Sr1–Hg	3.433(2)–3.723(3), 3.932(3)–4.136(3)	Hg8–Hg	2.879(2)–3.661(1)
Sr2–Hg	3.392(2)–3.884(3), 4.358(3)–4.670(3)	Hg9–Hg	3.063(1)–3.803(1)
Hg1–Hg	2.879(2)–3.803(1)	Hg10–Hg	2.973(2)–3.588(2)
Hg2–Hg	2.904(2)–3.621(1)	Hg11–Hg	2.999(2)–3.191(1)
Hg3–Hg	2.856(2)–3.621(1)	Hg12–Hg	2.904(2)–3.016(1)
Hg4–Hg	2.856(2)–3.471(2)	Hg13–Hg	2.879(2)–3.471(2)
Hg5–Hg	2.879(2)–3.717(2)	Hg14–Hg	2.947(1)–3.422(2)
Hg6–Hg	2.905(2)–3.717(2)	Hg15–Hg	2.882(2)–3.212(2)
Hg7–Hg	2.933(2)–3.661(1)	Hg16–Hg	2.947(1)–3.502(2)

<sup>a</sup> A distance cutoff of 4.0  $\text{\AA}$  was used; slightly longer distances around the coordination environment of Sr atoms are also indicated.



out with an improved tetrahedron method over 80 irreducible  $k$  points.

## Conclusions

The existence of the phase  $\text{SrHg}_8$ , first mentioned over 100 years ago, has been confirmed. Its structure is new and complex, built up from  $\text{Sr@Hg}_{18}$  clusters condensed in a three-dimensional framework. The formation of this compound supports the modifications proposed to the Sr–Hg phase diagram, including the likelihood that “ $\text{SrHg}_{13}$ ” does not exist.<sup>11</sup> Further work remains to clarify these details in the Hg-rich region of the phase diagram; in particular, the recent reformulation of “ $\text{Sr}_{14}\text{Hg}_{51}$ ” to  $\text{Sr}_{11-x}\text{Hg}_{54+x}$  places this phase,<sup>10</sup> and not  $\text{Sr}_{13}\text{Hg}_{58}$ , adjacent to  $\text{SrHg}_8$ .

## Acknowledgements

The authors acknowledge the Donors of the American Chemical Society Petroleum Research Fund for partial support of this research. We thank Dr Robert McDonald and Dr Michael J. Ferguson (X-ray Crystallography Laboratory) for assistance with the single-crystal X-ray data collection.

## References

- 1 H. J. Deiseroth, *Prog. Solid State Chem.*, 1997, **25**, 73–123.
- 2 H. J. Deiseroth, in *Molecular Clusters of the Main Group Elements*, ed. M. Driess and H. Nöth, Wiley-VCH, Weinheim, 2004, pp. 169–187.
- 3 C. Gumiński, in *Intermetallic Compounds: Principles and Practice*, ed. J. H. Westbrook and R. L. Fleischer, Wiley, Chichester, 2002, vol. 3, pp. 21–35.
- 4 A. V. Tkachuk and A. Mar, *Chem.–Eur. J.*, 2009, **15**, 10348–10351.
- 5 W. Kerp, *Z. Anorg. Chem.*, 1898, **17**, 284–309.
- 6 W. Kerp and W. Böttger, *Z. Anorg. Chem.*, 1900, **25**, 1–71.
- 7 A. Guntz and G. Roederer, *Bull. Soc. Chim. Fr.*, 1906, **35**, 494–503.
- 8 G. Devoto and E. Recchia, *Gazz. Chim. Ital.*, 1930, **60**, 688–692.
- 9 G. Bruzzone and F. Merlo, *J. Less Common Met.*, 1974, **35**, 153–157.
- 10 A. V. Tkachuk and A. Mar, *Inorg. Chem.*, 2008, **47**, 1313–1318.
- 11 C. Gumiński, *J. Phase Equilib. Diffus.*, 2005, **26**, 81–86.
- 12 L. Pauling, *The Nature of the Chemical Bond*, Cornell University Press, Ithaca, NY, 3rd edn, 1960.
- 13 A. Palasyuk, J.-C. Dai and J. D. Corbett, *Inorg. Chem.*, 2008, **47**, 3128–3134.
- 14 J. Donohue, *The Structures of the Elements*, Wiley, New York, 1974.
- 15 G. M. Sheldrick, *SHELXTL*, version 6.12, Bruker AXS Inc., Madison, WI, 2001.
- 16 L. M. Gelato and E. Parthé, *J. Appl. Crystallogr.*, 1987, **20**, 139–143.
- 17 R. Tank, O. Jepsen, A. Burkhardt and O. K. Andersen, *TB-LMTO-ASA Program*, version 4.7, Max Planck Institut für Festkörperforschung, Stuttgart, 1998.